# Density dependence revisited: strong evidence for superlinear population growth

James A. Orr*[1], Kaleigh E. Davis[1,2], Alicia H. Williams[1], Jan Engelstädter[1], Daniel B. Stouffer[3], and Andrew D. Letten*[1]

[1]School of the Environment, The University of Queensland, Brisbane, Queensland 4072, Australia
[2]Department of Integrative Biology, University of Guelph, Guelph, Ontario, Canada
[3]Department of Evolutionary and Integrative Ecology, Leibniz Institute of Freshwater Ecology and Inland Fisheries (IGB), Berlin, Germany

**Keywords:** Population dynamics, consumer-resource models, sublinear growth, functional response

**Data availability statement:** All the data and code associated with this study are available on GitHub at `https://github.com/jamesaorr/chemo-dd`.

## Abstract

Density dependence is a core principle in ecological and evolutionary theory, and yet the precise nature of the relationship between per capita growth and population size continues to ignite debate. While sublinear (convex/decelerating) density dependence is frequently observed in empirical studies, standard techniques for estimating density dependence are prone to unreliable inference. At the same time, the putative ubiquity of sublinearity in nature is at odds with the predictions of mechanistic models of resource competition. We used a continuous-culture approach, which bypasses the inferential challenges hindering conventional methods, in order to investigate the shape of density dependence in *Escherichia coli*. In agreement with the predictions of a model of resource competition empirically parameterised from independent growth assays, we found strong evidence for superlinear (concave/accelerating) density dependence. Despite the simplicity of our experimental system, we hypothesise that the evidence for sublinearity as a widespread phenomenon is less robust than widely assumed. Resolving this debate has significant implications for our fundamental understanding of ecosystem stability and the development of reliable models informing conservation and resource management.

*Correspondence: james.orr@uq.edu.au; a.letten@uq.edu.au

# Introduction

Density-dependent population growth is a fundamental principle in ecology and evolution, shaping both the generation and maintenance of biodiversity. For over a century, scientists have used phenomenological models of density dependence to help understand, predict, and manage populations of animals, plants, and microbes [1, 2]. The classic example is the logistic model, where per capita growth rate declines linearly with density. Few organisms, however, exhibit strictly linear density dependence. One pattern that is generally believed to predominate in nature is so-called 'sublinear' (i.e., decelerating) density dependence [2, 3], where per capita growth rate declines most rapidly at low densities. It is less widely appreciated that pure sublinearity runs counter to the predictions of mechanistic models of competition, which typically generate superlinear (i.e., accelerating) or more complex patterns of density dependence [4–6]. The extent to which this tension reflects a flaw in the theory or the data remains unclear.

A central empirical challenge in estimating the shape of density dependence is that in most systems it is impractical to hold densities constant while simultaneously observing resulting growth rates [4]. Exclusively studying organisms with discrete growth dynamics offers a partial solution, but the potential for decoupled effects of density on growth rate (e.g., due to delayed resource depletion) remains a problem [4, 7]. Both experiments and observational time-series are also plagued by statistical issues, with sublinearity potentially emerging as an artefact of regressing a noisy variable upon itself [8]. Sparse sampling can introduce a comparable bias [8], while inference from natural systems may also be compromised by the confounding effect of interspecific interactions [2]. Taken together, these empirical limitations cast doubt on the reliability of conventional methods for investigating density dependence.

To circumvent these problems, Abrams [4] proposed an alternative experimental approach that reverses the logic of traditional tests of density-dependence; instead of measuring per-capita growth rate over experimentally manipulated densities, the hypothetical experimenter manipulates harvest rates in order to observe their impact on equilibrium density (Fig. 1A) [4]. In a continuously harvested population, per capita growth rate is equal to the harvest rate at equilibrium, and therefore equilibrium density can be treated as a function of growth rather than the other way around [4, 7]. Inverting this function returns the familiar curve describing growth rate as a function of density, hence we term this technique 'growth-density inversion'. While Abrams recognised the impracticalities of implementing this approach in most natural systems, he employed the same logic to deduce the emergent shape of density dependence arising from classical consumer-resource models [4, 9]. Given saturating growth functions, consumer-resource models point to a greater prevalence of superlinear density dependence than the empirical data would suggest [4–6].

Building upon Abrams' insights, we used growth-density inversion to generate analytical predictions for the shape of density dependence in the model bacteria *Escherichia coli* via an empirically

parametrised consumer-resource model. We then implemented the technique experimentally, using a continuous-culture system to measure equilibrium densities under different dilution (i.e., harvesting) rates. This two-pronged approach combines the mechanistic insight afforded by a model-based prediction, with a fully empirical test of density dependence that bypasses the statistical and experimental artifacts of traditional methods.

## Results & Discussion

We used 143 independent growth assays for *E. coli* strain MG1655 across a range of initial glucose concentrations to parameterise a consumer-resource model assuming Monod growth dynamics (Fig. 1B). Solving the model for equilibrium density now assuming a range of continuous dilution (i.e., harvesting) rates predicted an acutely superlinear density-dependent function for *E. coli* (inset in Fig. 1B). To test this prediction, we then ran a series of independent chemostat experiments, growing replicate lines under equivalent dilution rates to those investigated analytically (until they established a stable equilibrium). Next, to quantify the strength and shape of density dependence, we fitted an inverse $\theta$-logistic model to equilibrium density as a function of dilution rate, where $\theta<1$, $\theta>1$ and $\theta=1$ corresponds to sublinear, superlinear and linear density dependence, respectively (see Methods and Supplementary Information for further methodological details). The experimental results aligned with the predictions of the consumer-resource model. More specifically, we found compelling evidence for superlinear density dependence, with $\theta = 4.39$ (95% credible intervals: 2.14-7.76) (Fig. 1C).

The role of the consumer's functional response in determining the shape of emergent density dependence is conspicuous in Fig. 1B. Abrams' principle of "inheritance of the curvature" posits that a consumer's density dependence will also be influenced by the shape of density dependence of the resource [4, 9]. In contrast to systems where resources grow logistically or enter in periodic pulses, continuous resource supply represents one of the few theoretical conditions under which regions of sublinear density dependence may arise [4–6]. In our experimental system, however, adjusting chemostat dilution rate, and therefore harvest rate, also meant changing the resource supply rate, a consequence of which is that the independent effect of the resource supply dynamic on the emergent shape of density dependence is cancelled out. We therefore also investigated the predictions of the empirically parameterised model under three alternative resource supply regimes (continuous, pulsed, and logistic) and three baseline mortality rates (25%, 50%, and 75% of the maximum growth rate). Under pulsed and logistic supply, the model predicts exclusively superlinear density dependence (centre and right columns in Fig. 2). Under continuous resource supply, the model predicts a switch from superlinearity to sublinearity as density increases (left column in Fig. 2), with the latter region only being conspicuous at low mortality rates.

The predicted absence of sublinearity at low densities (under any combination of resource dynamic and mortality) stands in contrast with a large body of theoretical and empirical research whose

conclusions derive from models characterised by sublinear density dependence. In a recent study [2], sublinearity at low density was a crucial factor fostering a presumptive positive relationship between diversity and stability [10]. Our findings are also at odds with the assumptions of sublinearity that underpin many population models that inform conservation and resource management decisions [11, 12]. It may be tempting to attribute this disconnect to the ecological simplicity of our bacterial study system or as a phenomenon that is more broadly unique to microbes. Indeed, a recent analysis of diverse microbial time-series (employing a novel statistical approach) also found no evidence for sublinear growth [13]. Nevertheless, we are unaware of any arguments from first principles why increasing organismal or system complexity should drive a universal switch from superlinearity to sublinearity. On the contrary, given the prevalence of saturating functional responses across diverse organisms [14], a reasonable prediction deriving from the principle of inheritance of the curvature [4] is that density dependence will only become increasingly superlinear with each jump in trophic level.

To our knowledge, this is the first study to directly compare predictions from empirically parameterised consumer-resource models with independent experimental observations of density dependence. The qualitative alignment we observe between model-predicted and experimentally observed density dependence (Figs. 1B & 1C insets, respectively) makes a compelling case for the explanatory power of even simple consumer-resource models, particularly given that the model was parameterised using independent batch culture data. That being said, the higher maximum growth rate observed under continuous culture conditions (y-intercept in Fig. 1C inset) suggests a potential plastic shift to a faster-growing phenotype at high dilution rates. Nevertheless, even without phenotypic plasticity, the $\theta$-logistic model is not usually flexible enough to capture the density-dependence that emerges from most consumer-resource models [4]. In natural systems, where a species' density dependence may be influenced by many biological processes (e.g., dispersal, species interactions), more flexible phenomenological models of density dependence that allow for contiguous sublinear and superlinear regions (e.g., the basic-Savageau model [15]) may be required to accurately describe population dynamics.

# Conclusion

In this study, we found strong evidence for superlinear density dependence that aligns with predictions from mechanistic theory, predictions that are general and taxonomically agnostic. When considered alongside the serious, yet widely ignored, biases introduced by conventional methods for estimating density dependence, we contend that the evidence supporting sublinear density dependence as a universal phenomenon may be far less robust than commonly assumed. Resolving this debate carries potentially significant implications, not only for our fundamental understanding of ecosystem stability and the maintenance of biodiversity, but also for the development of reliable population models that inform conservation and resource management strategies.

## Methods

We used 143 independent batch-culture growth assays of the model bacteria *Escherichia coli* (MG1655) to parameterize a consumer-resource model, and then used those parameters to predict the shape of density dependence for *E. coli* in continuous culture. We then empirically tested this prediction by growing *E. coli* populations in 30mL chemostats supplied with 0.05% glucose M9 media. Dilution rates were manipulated, and samples were taken daily until populations reached equilibrium. The shape of density dependence was quantified by fitting an inverse $\theta$-logistic model to the experimental data using (i) a grid-based Bayesian approach, which prevented predictions of negative densities (Fig. 1B) and (ii) a Bayesian model implemented in Stan via the brms R package, which used MCMC and constrained the estimated maximum growth rate to be greater than the highest observed growth rate (reported in the SI). The parameterized consumer-resource model was then used to predict the shape of density dependence under continuous, pulsed, and logistic resource supply regimes across three baseline mortality rates. Further details of the experiments and analyses are in the Supporting Information.


## Acknowledgements

ADL is supported by Australian Research Council grants DP220103350 and DE230100373. JAO and AHW are supported by Australian Research Council grant DE250100656.


## Author Contributions

ADL conceived the idea of the study. KED, JAO, and AHW performed the experiments. JAO analysed the data and made the figures with support from ADL, JE, and DBS. JAO and ADL wrote the first draft of the manuscript. All authors contributed to the final manuscript.

# References


[1] Pearl R, Parker SL (1922) On the influence of density of population upon the rate of reproduction in drosophila. *Proceedings of the National Academy of Sciences* 8(7):212–219.

[2] Hatton IA, Mazzarisi O, Altieri A, Smerlak M (2024) Diversity begets stability: Sublinear growth and competitive coexistence across ecosystems. *Science* 383(6688):eadg8488.

[3] Sibly RM, Barker D, Denham MC, Hone J, Pagel M (2005) On the regulation of populations of mammals, birds, fish, and insects. *Science* 309(5734):607–610.

[4] Abrams PA (2009) Determining the functional form of density dependence: deductive approaches for consumer-resource systems having a single resource. *The American Naturalist* 174(3):321–330.

[5] Fronhofer EA, Govaert L, O'Connor MI, Schreiber SJ, Altermatt F (2023) The shape of density dependence and the relationship between population growth, intraspecific competition and equilibrium population density. *Oikos* p. e09824.

[6] Letten AD (2025) Making sense of (sublinear) density dependence. *Trends in Ecology & Evolution*.

[7] Smith FE (1963) Population dynamics in daphnia magna and a new model for population growth. *Ecology* 44(4):651–663.

[8] Doncaster CP (2008) Non-linear density dependence in time series is not evidence of non-logistic growth. *Theoretical Population Biology* 73(4):483–489.

[9] Abrams PA (2022) *Competition theory in ecology*. (Oxford University Press).

[10] Aguadé-Gorgorió G, Lajaaiti I, Arnoldi JF, Kéfi S (2024) Unpacking sublinear growth: diversity, stability and coexistence. *Oikos* p. e10980.

[11] Brooks EN (2024) Pragmatic approaches to modeling recruitment in fisheries stock assessment: A perspective. *Fisheries Research* 270:106896.

[12] Koetke LJ, Duarte A, Weckerly FW (2020) Comparing the ricker and $\theta$-logistic models for estimating elk population growth. *Natural Resource Modeling* 33(4):e12270.

[13] Camacho-Mateu J, Lampo A, Castro M, Cuesta JA (2025) Microbial populations hardly ever grow logistically and never sublinearly. *Physical Review E* 111(4):044404.

[14] Jeschke JM, Kopp M, Tollrian R (2004) Consumer-food systems: why type i functional responses are exclusive to filter feeders. *Biological Reviews* 79(2):337–349.

[15] Ross J (2009) A note on density dependence in population models. *Ecological Modelling* 220(23):3472–3474.

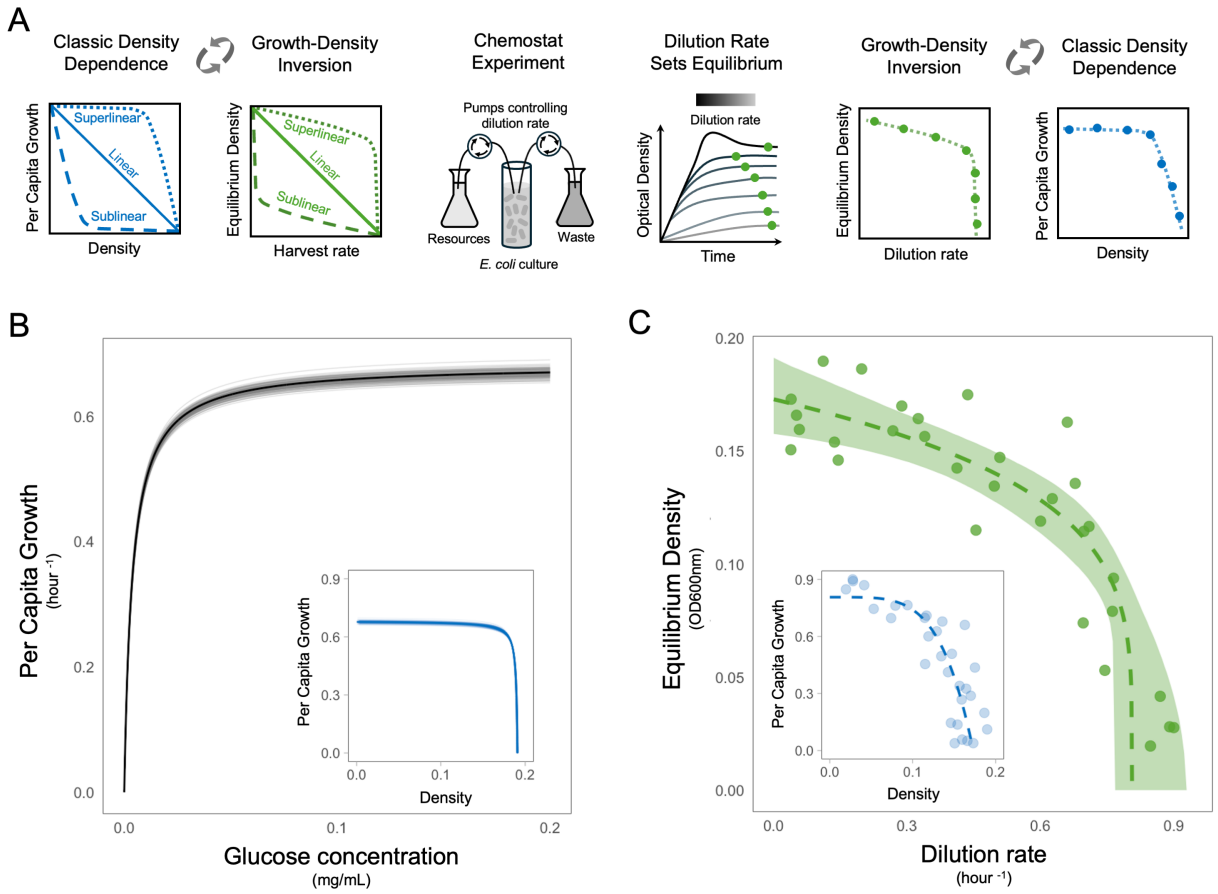


**Figure 1:** **(A)** Schematic of the experimental approach where the classic density dependence perspective (blue) is inverted (green) to overcome the challenges of manipulating densities. We varied the dilution rate of chemostats and quantified densities at equilibrium (when growth rate is equal to dilution rate) to study the shape of density dependence. **(B)** Parameterized Monod growth function with 100 posterior draws representing uncertainty. Inset shows the analytical prediction for the density dependence of this parameterized consumer–resource model. **(C)** Inverse $\theta$-logistic model fitted to the experimental data with 95% credible intervals. Inset shows the same data and model with axes inverted to give the classic density dependence perspective.

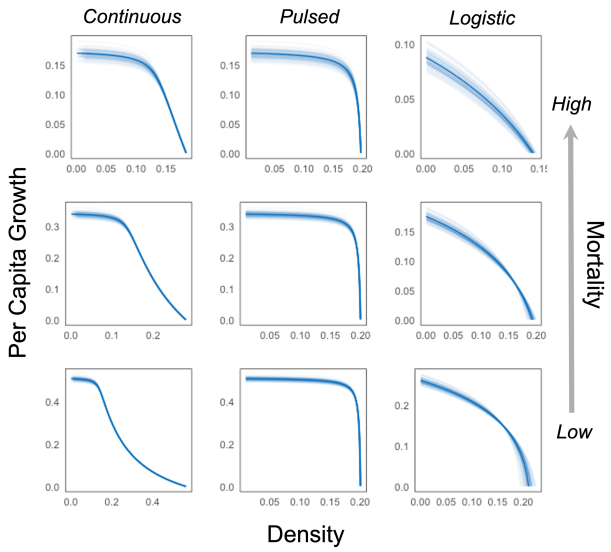


**Figure 2:** Predicted density dependence across three resource supply regimes (columns) and three baseline mortality rates (rows). Thick lines show predictions using median parameter estimates and thin lines are 100 posterior draws representing uncertainty.

# Supporting Information for

# Density dependence revisited: strong evidence for superlinear population growth

James A. Orr[1], Kaleigh E. Davis[1,2], Alicia H. Williams[1], Jan Engelstädter[1], Daniel B. Stouffer[3], and Andrew D. Letten[1]

[1]School of the Environment, The University of Queensland, Brisbane, Queensland 4072, Australia
[2]Department of Integrative Biology, University of Guelph, Guelph, Ontario, Canada
[3]Department of Evolutionary and Integrative Ecology, Leibniz Institute of Freshwater Ecology and Inland Fisheries (IGB), Berlin, Germany

## Contents

# S1 Modelling resource-dependent consumer growth

## S1.1 Batch culture data

Growth curves were obtained for *E. coli* strain MG1655 across a range of initial glucose concentrations. For each replicate, an overnight culture was grown at 37 °C in M9 media supplemented with 0.05% glucose for 18 hours. 1mL of culture was then pelleted and resuspended in 200uL M9 0% glucose in order to remove any residual glucose. 2$\mu$L of this resuspension was subsequently inoculated into 178$\mu$L of M9 with ten different glucose concentrations ranging from 0-0.01% glucose in a 96-well plate maintained at 37 °C. Optical density measurements were made every minute in a Epoch 2 plate reader over 24 hours. Owing to the appearance of two distinct growth phases (likely attributable to a diauxic shift from the primary glucose substrate to a carbon intermediate), we truncated the growth curve to only include the first, glucose limiting phase of growth. Each glucose concentration was replicated 15 times for a total of 150 individual assays (seven were subsequently excluded due to contamination or irregular OD measurements).

## S1.2 Model formulation and parameterization

Based on the prevailing literature, we assumed that *E. coli* in batch culture should show resource-dependent growth that follows a Monod or Michaelis–Menten relationship (i.e., growth rate saturates at high resource concentrations) [1]:

$$\frac{dN}{dt} = \frac{\mu_{\max} R}{k_S + R} N \,, \tag{S1}$$

where $N$ is the consumer biomass density, $R$ is the resource concentration, $\mu_{\max}$ is the maximum growth rate and, and $k_S$ is the half-saturation constant. In parallel to the equation for consumer growth, there is a corresponding equation for resource depletion given by

$$\frac{dR}{dt} = -\frac{1}{\upsilon} \frac{\mu_{\max} R}{k_S + R} N \,, \tag{S2}$$

where $\upsilon$ is the yield of consumer density produced per one unit of resource concentration taken up.

Upon noting that the quantity $K(t) = N(t) + \upsilon R(t)$ is actually constant for all times because $\frac{dK}{dt} = \frac{dN}{dt} + \upsilon \frac{dR}{dt} \equiv 0$ given both Eq. S1 & S2, it is possible to use a "conservation approach" to describe the consumer dynamics [2]. This allows us to eliminate $R$ from Eq. S1 to give

$$\frac{dN}{dt} = \frac{\mu_{\max} (K - N)}{\upsilon k_S + K - N} N \,. \tag{S3}$$

This conversation approach further implies that $K \equiv N_0 + \nu R_0$, where $N_0$ is the initial consumer biomass density and $R_0$ is the initial resource concentration. The full set of parameters needed to predict growth dynamics is $\{N_0, R_0, \mu_{\max}, k_S, \upsilon\}$.

Since the initial inoculum densities deriving for each of the 15 overnight cultures potentially varied between themselves, we treated each of these 15 values as additional unknowns when fitting the model to the observed data [3]. Optical density measurements are also subject to variation due directly to the M9 growth media. To account for this as well as non-independence across observations, we allow the OD due to growth media to vary

randomly across 96-well plates and across wells nested within plates using a hierarchical model. We furthermore assumed that the total optical density in a well was the sum of the optical density due to the growth media and the optical density due to the consumer biomass.

We estimated the model parameters via Bayesian inference using the `sample()` method from the `cmdstanr` package v0.9.0 [4] in `R` v4.5.1 [5]. We sampled over four chains with 1000 warmup and 1000 post-warmup Hamiltonian Monte Carlo iterations, resulting in a total of 4000 posterior samples. To promote chain convergence, we set the `max_treedepth` parameter to 20 and the `adapt_delta` parameter to 0.999. We solved the initial-value problem using the `ode_rk45()` method in Stan [6]. All unknown parameters were constrained to be positive in order to keep the model biologically sensible. The full Bayesian description of our model including prior distributions is

$$\begin{aligned}
\mathrm{OD}_{pwt} &\sim \mathrm{Lognormal}\left(\ln \lambda_{pwt}, \sigma_{\mathrm{OD}}\right) && \text{(S4)}\\
\lambda_{pwt} &= N_{pwt} + b_{pw} && \text{(S5)}\\
N_{pwt} &= \texttt{ode_rk45}\left(N_{0,p}, t, K_{pw}, \mu_{\max}, k_S, \upsilon\right) && \text{(S6)}\\
K_{pw} &= N_{0,p} + \upsilon R_{0,pw} && \text{(S7)}\\
\ln b_{pw} &= \beta_{pw} && \text{(S8)}\\
\{\ln N_{0,1}, \ldots, \ln N_{0,15}\} &\sim \mathrm{Normal}(0, 1) && \text{(S9)}\\
\{\ln \mu_{\max}, \ln k_S, \ln \upsilon\} &\sim \mathrm{Uniform}(-\infty, \infty) && \text{(S10)}\\
\beta_0 &\sim \mathrm{Uniform}(-\infty, \infty) && \text{(S11)}\\
\beta_p &\sim \mathrm{Normal}(\beta_0, \sigma_p) && \text{(S12)}\\
\beta_{pw} &\sim \mathrm{Normal}(\beta_p, \sigma_w) && \text{(S13)}\\
\{\sigma_{\mathrm{OD}}, \sigma_p, \sigma_w\} &\sim \text{Student-}t(3, 0, 2.5) && \text{(S14)}
\end{aligned}$$

where for convenience we have introduced the subscript $p$ to denote the 96-well plate, the subscript $w$ to denote the well in that plate, and the subscript $t$ to denote the time elapsed at the moment of estimating optical density.

## S1.3 Prediction of density dependence

We then used the parameterized consumer-resource model to predict the shape of density dependence in our experiment. Though the parameters were inferred from batch culture, we can also use those same parameters to predict consumer behaviour in other contexts. We started from a consumer-resource model for one resource (glucose) and one consumer (*E. coli*) with Monod growth and chemostat resource supply:

$$\begin{aligned}
\frac{dN}{dt} &= N\left(\frac{\mu_{\max} R}{k_S + R} - m\right)\\
\frac{dR}{dt} &= d(S - R) - \frac{\mu_{\max} R}{k_S + R} QN
\end{aligned} \qquad \text{(S15)}$$

where $N$ is the consumer density, $R$ is the resource concentration, $\mu_{\max}$ is the maximum growth rate, $k_S$ is the half saturation constant, $m$ is the mortality rate, $d$ is the dilution rate, $S$ is concentration of glucose in the supply, and $Q$ is the quota (i.e., resources per consumer), which is the inverse of the yield parameter used above.

We had empirical estimates for $\mu_{\max}$, $k_S$, and $Q$ (see above), and we knew the value of $S$ in our system. Following Abrams [7, 8], we could therefore analytically predict the relationship between per capita growth rate and equilibrium density:

$$N^* = \frac{d}{\mu_{\max} Q}\left[\frac{\mu_{\max} S}{m} - \frac{m k_S}{\mu_{\max} - m} - k_S\right] \tag{S16}$$

To predict the density dependence observed in our experiment, we inserted median parameter estimates (and posterior draws for uncertainty) into Eq. S16 and we set $m = d$ (assuming washout was the dominant source of loss).

# S2 Growth-density inversion

Traditional tests of density dependence, where species densities are manipulated (often to unrealistic levels) and resulting growth rates are quantified, suffer from time delay issues [7, 9]. Specifically, delayed effects of density on growth rate distorts the shape of density dependence and keeping densities fixed is impossible for many systems. Given these challenges, an alternative test of density dependence was proposed by Peter Abrams [7, 8]. This intuitive approach, which we call "growth-density inversion", reverses the logic of traditional tests of density-dependence by manipulating per capita growth and quantifying resulting densities. In practice, this entails varying harvest rate and quantifying densities once equilibrium is reached (when harvest is equal to growth).

Here, we studied the density dependence of *Escherichia coli* by manipulating the dilution rate of chemostats and quantifying bacterial population density at equilibrium (when growth rate equals dilution rate). Bacterial populations growing in chemostats is an ideal first empirical application of the growth-density inversion approach as steady state equilibria are reached (cycling population dynamics would complicate the analysis), and the short generation time of microbes facilitates observation of population density responses to changes in per capita growth rates.

In Abrams' analytical work, density dependence is studied by varying "neutral parameters", which only directly impact a focal species [8]. However, experimentally manipulating a "neutral parameter" of the bacteria in a chemostat system, such as harvest rate, is a technical challenge. While dilution rate is not a "neutral parameter", in the sense that it directly impacts both the bacteria and the resources, it offers a feasible way to manipulate bacteria harvest rate, and we can analytically control for the effect it has on resource dynamics. A consumer's density dependence is influenced by the shape of its functional response and by the density dependence of the resource it consumes [7, 10, 11, 12]. By manipulating dilution rate we effectively observed how the bacteria's functional response shapes their density dependence independently of resource dynamics.

# S3 Experimental procedure

Five experimental replicates were performed using a "Chi.Bio" chemostat system comprised of eight 30mL reactors connected to a series of peristaltic pumps. The reactors were held at constant temperature with continuous stirring and measurement of optical density measurement (600nm) at 1-minute intervals. In each run of the experiment, we tested

six different dilution rates (that varied across experimental replicates), in addition to one methodological control (*E. coli* grown at the same dilution rate across experimental replicates) and one biological control (sterile media).

The day before an experimental replicate, the reactors, tubing, and media bottles of the chemostat system were autoclaved, 0.05% glucose M9 media was prepared, and an overnight culture of *E. coli* was set up at 37 °C shaking at 180 rpm. Once the overnight culture had grown for 18 hours, reactors with 20mL media were inoculated with 1mL of the overnight culture (or 100$\mu$L in the first two experimental replicates). All reactors were set to the same temperature (37 °C), stirring rate, and outflow rate. The inflow rates of the reactors varied in order to experimentally manipulated dilution rate (and therefore bacteria harvest rate). When the inflow pumps ran, fresh media entered the reactors and raised the level of the liquid above the outflow port. After several minutes of stirring, the outflow pumps ran until the level of the liquid in all reactors returned to the level of the outflow port. The inflow and outflow pumps ran every 20 minutes at fixed dilution rates that varied depending on inflow rates.

The chemostats were sampled each day for up to four days and the experiments ran until the populations were inferred to have reached equilibrium (based on the live optical density read-out). The higher the dilution rate, the longer it took the populations to reach equilibrium. For sampling, 0.5ml of liquid was collected from the outflow ports of the reactors using syringes. 200$\mu$L of this was used to obtain higher precision optical density readings with a plate reader and 100$\mu$L was diluted and then plated onto LB agar for colony counting.

## S3.1 Calculating dilution rates

In classic chemostat theory, the dilution rate is defined as the volume of fresh media supplied per unit time divided by the volume of the culture. This assumes continuous flow, with instantaneous inflow and outflow, such that the volume of the culture is constant. In practice, however, chemostat systems often have discrete pulses of inflow and outflow, resulting in transient variation in culture volume. In our system, fresh media was added every 20 minutes and there was approximately two minutes intentionally left between inflows and outflows to allow for thorough mixing.

To calculate a continuous dilution rate in our system with discrete pulses we calculated the exponential decay rate that would have produced the same net dilution over a full inflow-outflow cycle. A single inflow pulse dilutes the population as follow:

$$N_1 = N_0 \cdot \frac{V_0}{V_0 + V_{in}} \tag{S17}$$

where $V_0$ is the baseline culture volume (21mL) and $V_{in}$ is the inflow volume (equal to the outflow volume, which we measured daily). We can then match this discrete dilution factor to a continuous exponential decay model over a full cycle:

$$N_0 \cdot \frac{V_0}{V_0 + V_{in}} = N_0 \cdot e^{-d\tau} \tag{S18}$$

where $\tau$ is the length of the inflow-outflow cycle (20 minutes) and $d$ is the dilution rate.

After rearranging we have:

$$d = \frac{\log(\frac{V_0+V_{in}}{V_0})}{\tau} \tag{S19}$$

This allowed us to obtain a dilution rate that we could use for continuous-time modelling that reflected the effects of the discrete inflow and outflow pulses in our system.

## S3.2 Determining when populations were at equilibrium

Although samples were taken every day, only samples taken when populations were at equilibrium were used to estimate the shape of density dependence. Three biological phenomena needed to be considered when determining if a population had reached equilibrium: 1) populations under higher dilution rates took longer to reach equilibrium; 2) populations under the lowest dilution rates exhibited overshooting dynamics where density initially exceeded their equilibrium density before settling back down; 3) there was a risk of adaptive evolution to the different dilution rates through the course of the experiment.

Based on these factors, we used simple heuristics to determine when populations were at equilibrium. For the lowest dilution rates, samples taken on day four were considered at equilibrium to account for the overshooting dynamics (this was in line with previous work with this system). For the intermediate dilution rates, samples taken on days one and two were considered at equilibrium as there was no overshooting dynamics but there was a risk of evolution to experimental conditions (as evidenced by jumps in OD after a period of stabilisation). For the highest dilution rates, samples taken on days three and four were considered at equilibrium as populations were still increasing on days one and two. No samples taken after day four were used due to the increased risk of evolutionary change. All dilution rates below 0.1 mL/hour/mL were treated as "low" dilution rates; optical density always decreased from day one to day four in these populations (overshoot). All dilution rates above 0.65 mL/hour/mL were treated as "high" dilution rates; optical density always increased from day one to days three/four in these populations. Dilution rates between 0.1 and 0.65 mL/hour/mL were treated as "intermediate" dilution rates; populations reached equilibrium by day one according to the "Chi.Bio" timeseries.

Five experimental replicates each with eight reactors gave us forty individual reactors. After removing the biological controls (no bacteria present), a reactor whose pump failed, and reactors that were not sampled on the days when their populations were considered at equilibrium, we were left with 31 reactors that had at least one sample taken when populations were at equilibrium. 15 reactors had two samples taken (on two separate days) when populations were at equilibrium, giving 46 observations in total. For these 15 reactors, we took the average optical densities of the two samples taken. As demonstrated in the R notebooks at `https://github.com/jamesaorr/chemo-dd`, our results are insensitive to these data processing choices. Indeed, broadly ignoring the heuristics (e.g., by only considering samples from days three or four), changing the cutoff for what was considered "low", "intermediate", or "high" dilution rates, or using the first or last equilibrium sample rather than the average, all return data showing superlinear density dependence.

# S4 Estimating the shape of observed density dependence

The $\theta$-logistic model is the canonical model for describing the shape of density dependence in ecology [13, 8, 14]. It extends the logistic model by including an additional parameter to control the non-linearity of the relationship between per capita growth and density:

$$g = r\left(1 - \left(\frac{N}{K}\right)^{\theta}\right) \tag{S20}$$

where $g = \frac{1}{N}\frac{dN}{dt}$ is the per capita growth, $N$ is the population density, $r$ is the maximum (intrinsic) growth rate, $K$ is the carrying capacity, and $\theta$ controls the shape of density dependence. When $\theta > 1$, density dependence is superlinear; when $\theta < 1$, it is sublinear; and $\theta = 1$ recovers the classic logistic model. For our "Growth-Density Inversion" experimental approach, per capita growth (dilution rate) was our explanatory variable, and density was our response variable. We therefore fit an inverse $\theta$-logistic model to our data [7], which explained equilibrium density as a function of per capita growth:

$$N^* = K\left(1 - \frac{g}{r}\right)^{\frac{1}{\theta}} \tag{S21}$$

We first used the brms R package [15] to fit the inverse $\theta$-logistic model (Eq. S21) to our data with a Gamma distribution and an identity link function since equilibrium densities cannot be negative. Broad but biologically plausible priors were chosen for $r$ (uniform distribution between 0.6 and 1.1) and $K$ (uniform distribution between 0.15 and 0.25) based on growth rates and densities previously observed in this system. We set very loose priors for $\theta$ (uniform distribution between -1 and 10) ranging from highly sublinear to highly superlinear as this was the key parameter we were interested in estimating from the data.

The posterior estimates of this model were: $K = 0.20$ (95% credible interval: 0.17 to 0.23), $r = 0.93$ (0.90 to 0.99), and $\theta = 1.94$ (1.35 to 2.68), indicating superlinear density dependence. Although the posterior predictive checks were reasonably good, the posterior distribution of $r$ was bounded and negatively correlated with $\theta$. As seen in Eq. S21, the model becomes undefined when the maximum growth rate ($r$) is less than the largest observed dilution rate ($g$). Thus, the model cannot explore the region of parameter space where $r < g$. Incorporating measurement error in $g$, log-transforming the model, or reparametrizing the model could not resolve this boundary issue.

To overcome this limitation in the fitting of the model, we reverted to a grid-based Bayesian approach that was feasible given the low dimensionality of our model. We slightly modified Eq. S21 by bounding the function at $N^* = 0$ when $g \geq r$:

$$N^* = K\left(\max\left\{0, 1 - \frac{g}{r}\right\}\right)^{\frac{1}{\theta}} \tag{S22}$$

This equation gives the globally stable equilibrium population size, which is given by Eq. S21 for $r > g$ and zero otherwise. Thus, Eq. S22 ensured that the model was

well-defined over the full parameter space, including where $g \geq r$. A large grid was used with all combinations of 50 values of $K$, 50 values of $\theta$, 50 values of $r$, and 20 values of the standard deviation of the residual errors. The number of values for each parameter included in the grid was chosen to obtain relatively smooth posterior distributions for each parameter. The posterior probability of each combination of these parameters ($n = 2.5$ million) was calculated by combining the likelihood and the priors (same priors as the brms approach above). Randomly drawing combinations of parameters from the grid weighted by their posterior probability allowed us to obtain posterior draws and posterior predictive distributions.

The posterior estimates obtained from this grid-based Bayesian approach were: $K = 0.17$ (95% credible interval: 0.16 to 0.19), $r = 0.80$ (0.77 to 0.93), and $\theta = 4.39$ (2.14 to 7.76), again indicating superlinear density dependence. There was some evidence of bimodality in the posteriors of $r$ and $\theta$, reinforcing the idea that the $\theta$-logistic model is often not flexible enough to capture the true shape of density dependence, even for monotonic relationships. Irrespective of the data processing and modelling approaches used (see R notebooks at `https://github.com/jamesaorr/chemo-dd`), there was no qualitative change in the result; our experimental data showed superlinear density dependence.

# S5 Density-dependence predictions for other resource dynamics

We used the parametrized Monod function (see S1) to predict the shape of density dependence in resource supply regimes that weren't tested in our continuous-culture experiment. Median parameter estimates were used to make the predictions with posterior draws used to represent uncertainty.

To predict the shape of density dependence under chemostat resource supply (where harvest of bacteria is separated from resource dynamics), we parametrized Eq. S16 and examined how $N^*$ changed in response to varying harvest rate ($m$, a "neutral parameter"), while keeping dilution rate ($d$) fixed.

For logistically growing resource, we started with the consumer-resource model:

$$\begin{aligned} \frac{dN}{dt} &= N\left(\frac{\mu_{\max} R}{k_S + R} - m\right) \\ \frac{dR}{dt} &= rR\left(1 - \frac{R}{K}\right) - \frac{\mu_{\max} R}{k_S + R} QN \end{aligned} \tag{S23}$$

where $r$ is the intrinsic rate of growth of the resource and $K$ is the carrying capacity of the resource, and we could again analytically predict the shape of density dependence as:

$$N^* = \frac{k_S r[K\mu_{\max} - (k_S + K)m]}{Kq(m - \mu_{\max})^2} \tag{S24}$$

To obtain stable equilibria over a range of consumer mortality values in this model, a relatively low value of $K$ (0.0004) and a relatively high value of $r$ (100) were used to avoid cyclic dynamics or extinctions.

To estimate the shape of density dependence under pulsed resource dynamics we took a numerical approach, as Abrams' analytical technique is best suited to systems with fixed point equilibria. We simulated a consumer-resource system with Monod resource uptake and introduced resources as periodic pulses (with no resource loss other than through consumption). For each time step, we extracted per capita growth rate from the model and plotted this against consumer density. The magnitude and the frequency of the resource pulses has no impact on the shape of the consumer's density dependence as the resource itself has no density dependence (unlike logistic or continuous resources).

Finally, to illustrate the importance of baseline mortality rates in determining the shape of density dependence, we plotted the observed density dependence for each of the three resource supply regimes under baseline mortality rates of 25%, 50%, and 75% of the maximum growth rate.

# References


[1] Jacques Monod. The growth of bacterial cultures. *Annual Review of Microbiology*, 3(1):371–394, 1949.

[2] Rui Dilao and Tiago Domingos. A general approach to the modelling of trophic chains. *Ecological Modelling*, 132(3):191–202, 2000.

[3] Richard McElreath. *Statistical rethinking: A Bayesian course with examples in R and Stan*. Chapman and Hall/CRC, 2018.

[4] Jonah Gabry, Rok Češnovar, Andrew Johnson, and Steve Bronder. *cmdstanr: R Interface to 'CmdStan'*, 2025. R package version 0.9.0, https://discourse.mc-stan.org.

[5] R Core Team. *R: A Language and Environment for Statistical Computing*. R Foundation for Statistical Computing, Vienna, Austria, 2023.

[6] Bob Carpenter, Andrew Gelman, Matthew D Hoffman, Daniel Lee, Ben Goodrich, Michael Betancourt, Marcus Brubaker, Jiqiang Guo, Peter Li, and Allen Riddell. Stan: A probabilistic programming language. *Journal of statistical software*, 76:1–32, 2017.

[7] Peter A Abrams. Determining the functional form of density dependence: deductive approaches for consumer-resource systems having a single resource. *The American Naturalist*, 174(3):321–330, 2009.

[8] Peter A Abrams. *Competition theory in ecology*. Oxford University Press, 2022.

[9] Frederick E Smith. Population dynamics in daphnia magna and a new model for population growth. *Ecology*, 44(4):651–663, 1963.

[10] Emanuel A Fronhofer, Lynn Govaert, Mary I O'Connor, Sebastian J Schreiber, and Florian Altermatt. The shape of density dependence and the relationship between population growth, intraspecific competition and equilibrium population density. *Oikos*, page e09824, 2023.

[11] Sara A Reynolds and Chad E Brassil. When can a single-species, density-dependent model capture the dynamics of a consumer-resource system? *Journal of Theoretical Biology*, 339:70–83, 2013.

[12] Andrew D Letten. Making sense of (sublinear) density dependence. *Trends in Ecology & Evolution*, 2025.

[13] Michael E Gilpin and Francisco J Ayala. Global models of growth and competition. *Proceedings of the National Academy of Sciences*, 70(12):3590–3593, 1973.

[14] Ian A Hatton, Onofrio Mazzarisi, Ada Altieri, and Matteo Smerlak. Diversity begets stability: Sublinear growth and competitive coexistence across ecosystems. *Science*, 383(6688):eadg8488, 2024.

[15] Paul-Christian Bürkner. brms: An r package for bayesian multilevel models using stan. *Journal of statistical software*, 80:1–28, 2017.